

Mass transfer enhancement through Marangoni instabilities during single drop formation

M. Wegener^{*}, A.R. Paschedag[†], M. Kraume

Chair of Chemical Engineering, Technische Universität Berlin, Ackerstraße 71-76, D-13355 Berlin, Germany

[†] *University of Applied Science Berlin, Luxemburger Str. 10, D-13353 Berlin, Germany*

Abstract

The impact of Marangoni convection on the extraction efficiency during the drop formation stage is investigated in the system toluene/acetone/water for different initial solute concentrations and different drop diameters. Both mass transfer directions of the solute have been considered. Marangoni instabilities are supposed to increase the internal mixing and thus enhance mass transfer coefficients. Experimental results show a strong dependency on the mass transfer direction. The amount of solute extracted is between 19% and 55%. The total transferred mass M_A increases with drop diameter and initial concentration. Present models from the literature which predict extraction efficiencies do not take into account interfacial effects like Marangoni convection. A correlation is proposed introducing an effective diffusivity which depends on the initial solute concentration. The diffusivity factor increases linearly with initial solute concentration and is more sensitive in the mass transfer direction $c \rightarrow d$.

Keywords: drop formation, extraction, Marangoni convection, mass transfer

Nomenclature

A	area (m ²)
c	concentration (g/L)
d	diameter (mm)
D	diffusivity (m ² /s)
E	extraction efficiency
k	a constant
m	distribution coefficient
M	mass (μg)
n	a constant
R^2	correlation coefficient
v_N	dispersed phase nozzle velocity (m/s)
t	time (s)

Greek symbols

α	diffusivity factor
μ	dynamic viscosity (Pa·s)

^{*}Corresponding author. Tel.: +49 30 314 72791; fax: +49 30 314 21134.
E-mail addresses: mirco.wegener@tu-berlin.de (M. Wegener),
anja.paschedag@tfh-berlin.de (A.R. Paschedag),
matthias.kraume@tu-berlin.de (M. Kraume).

ρ density (kg/m³)
 σ interfacial tension (N/m)

Dimensionless numbers

Re_N nozzle Reynolds number $\frac{v_N d_N \rho}{\mu}$

Subscripts

0 initial
 A solute
 c contact
 f formation
 N nozzle
 P particle, drop

1. Introduction

The mass transfer of a solute between a dispersed and a continuous phase is a basic process in liquid-liquid extraction. A fundamental knowledge of the relevant physical phenomena during mass transfer is needed to predict mass transfer coefficients reliably. But this task is complex and subject to uncertainty since the manifold interactions during the different stages of the mass transfer process are not fully understood. These stages are in general [1-3]:

1. drop formation at a nozzle or spray tip,
2. free drop rise or fall in the continuous phase after release,
3. drop coalescence.

Every stage is more or less relevant depending on the type of column used. Drop formation and coalescence are more relevant in columns with internals and thus short free path length, the convection dominated free rise or fall is more significant, e.g. in spray columns [2].

Most of the models for the mass transfer coefficients proposed in the literature concern the free rise or fall stage. With these models, mass transfer coefficients or Sherwood numbers can be calculated, neglecting in most cases either the mass transfer resistance in the continuous phase or in the dispersed phase. Comparisons between experimental results and model predictions sometimes show unacceptable deviations [4]. One reason is the uncertain determination of the relevant mean initial drop solute concentration which depends on the drop formation process and which varies strongly with small changes between two experiments [5]. Experimental results in drop formation experiments show that 10-50% [1, 6-8] and in some cases up to 80% [9] of the total mass transfer can be completed after drop formation. Therefore, a model-based prediction of the drop formation process in combination with reliable experimental results is necessary.

Much experimental effort has been made in order to investigate the mass transfer rate during the drop formation [10]. Different experimental approaches have been established such as extrapolation methods to zero formation time or zero column height, the formation-collapse technique where the drop is withdrawn after formation by the same nozzle, or using short column heights (see literature cited in Walia

& Vir [11]). Every method has its advantages and shortcomings and is therefore subject to uncertainties [11, 12] since many experimental difficulties arise due to short time and length scales [10].

Most of the analytically derived models proposed in literature, e.g. [7, 13-16], are based on the unsteady-state diffusion theory using different approaches to describe the hydrodynamics of the process. They assume diffusion control and do not take into account internal circulation. Popovich *et al.* [17] showed that the total transferred mass M_A calculated by these models can be described with Eq. (1) if the spherical droplet grows uniformly with time:

$$M_A = \text{const} \cdot d_{p,f}^2 \Delta c_A \sqrt{t_f \pi D_A} \quad (1)$$

with the droplet diameter $d_{p,f}$ after drop formation time t_f , the concentration difference Δc_A between the initial solute concentration $c_{A,0}$ inside the drop and the equilibrium concentration in the drop for $t \rightarrow \infty$. The constant varies according to the different assumptions used in the models between the lowest value 6/7 (Licht & Pansing, [7]) and 24/7 (Heertjes *et al.* [16]). The extraction efficiency E is obtained if the transferred mass is divided by the maximum possible mass to be extracted, $V_p \Delta c_A$, and thus is independent of the initial solute concentration:

$$E = \text{const}_2 \cdot \frac{\sqrt{t_f D_A}}{d_{p,f}} \quad (2)$$

with $\text{const}_2 = 36/7\sqrt{\pi}$ for the model of Licht & Pansing and $\text{const}_2 = 144/7\sqrt{\pi}$ for the Heertjes *et al.* model. The constants for other models can be found in Walia & Vir [11].

Other aspects affecting the mass transfer efficiency which are not represented by Eqs. (1) and (2) are the influence of surfactants [8, 18], mass transfer direction, influence of drop release and the daughter drop remaining at the tip of the nozzle [2]. Liang & Slater [8] propose a circulation/diffusion model with two empirical parameters. The first accounts for the onset of internal circulation, the second one is used to formulate an overall effective diffusivity which accounts, e.g. for surface blockage due to surfactants. The model shows some success but also failures when compared to experimental data with small drop formation rates.

Interfacial instabilities occur if the local solute concentration varies along the interface. This leads to gradients of the interfacial tension which initiate interfacial convection (Marangoni convection). Thornton *et al.* [19], Thornton [20] and Javed *et al.* [21] found experimentally in the toluene/acetone/water system that interfacial instabilities significantly promote mass transfer rates in forming drops. Using a photochromic dye tracer technique they showed that Marangoni convection leads to surface renewal. This process is strongly time-dependent: mass transfer coefficients start from a high value and decrease with drop interface age. The initial mass transfer coefficient increases with higher initial solute concentrations. Much experimental work concerns interfacial instabilities at drops, e.g. in binary systems with or without surfactants [22-24], hanging drops [25] or rising/falling drops in a continuous phase [26, 27] in ternary systems. In all of these studies, Marangoni effects led to mass transfer enhancement. An increase in initial solute concentration usually increases the intensity of Marangoni induced flow patterns. Especially during drop formation, the concentration gradient is very high. Therefore, Marangoni convection is particularly

strong in this part of the process. Surfactants generally (but not always, see [23]) decrease the mass transfer rate, so clean conditions are necessary to observe Marangoni effects.

In the present study, drop formation experiments were conducted in a clean toluene/acetone/water system. Besides the drop diameter, initial solute concentration and mass transfer direction have been varied to account for the impact of Marangoni convection on the extraction efficiency. In this work, a short column with negligible time of drop rise and small coalescence area has been used. The transferred amount of the solute is measured collecting a defined number or volume of drops. The extraction efficiency which is determined by the experiment is then compared with models from literature (Eq. (2)). As discussed above, the models do not take into account the effect of Marangoni convection on the transferred mass. The present study deals with the question, in which manner Eq. (1) can be extended in order to account for the impact of solute concentration on mass transfer. It is proposed to introduce an effective diffusivity for both mass transfer directions in Eq. (1) which depends on the initial solute concentration.

2. Experimental detail

2.1 Experimental setup

Fig. 1 shows the experimental setup. It consists of a glass column with an inner diameter of 50 mm and a total height of 150 mm. Inside the column, a Teflon device (2) is mounted to collect the drops by promoting coalescence. The Teflon tip is jacketed by a glass cylinder (inner diameter 5 mm) to restrict the coalescence area to a minimum. The dispersed phase is stored in a storage vial (7). A Hamilton[®] PSD/2 module (5a) is used to generate drops of a specified volume (9) at a glass nozzle made by Hilgenberg[®] (inner diameter 0.5 mm). The volumetric flow rate of the pump is kept constant for all experiments to guarantee a constant nozzle Reynolds number ($Re_N \approx 16$). Drop release is accomplished automatically by a solenoid device (4), 0.2 s after the end of drop formation. When the drop is released, it coalesces nearly immediately at the Teflon tip. The distance between the Teflon tip and the upper edge of the drop is 3 mm in all experiments. The second pump (5b) withdraws the dispersed phase which is collected in a sample vial (8). The concentration measurements of the amount of acetone in the dispersed phase were performed using an Agilent[®] 7890A gas chromatograph. The whole procedure is computer controlled (6).

The standard test system toluene_(d)/acetone_(A)/water_(c) (*d*: dispersed phase, *A*: solute, *c*: continuous phase) as recommended by the European Federation of Chemical Engineering [28] has been used. For physical properties also see [29]. The system is highly sensitive to impurities and quality of the chemicals, thus only chemicals of high purity have been used (toluene p.a. $\geq 99.9\%$, acetone p.a. $\geq 99.8\%$ by Merck[®], deionized water with a specific resistance of 18.3 M Ω ·cm). Only the materials PTFE, glass and stainless steel were used. The column and all other relevant parts were cleaned mechanically and rinsed intensely before use. In every experiment, toluene and water were mutually saturated in order to avoid additional mass transfer.

Position of Fig. 1

2.2 Experiments

Five different drop diameters (2.0, 2.5, 3.0, 3.5, 4.0 mm) and five initial solute concentrations have been investigated in this study (see Table 1). Both mass transfer directions of acetone ($d \rightarrow c$ and $c \rightarrow d$) were investigated. The ratio of the initial solute concentrations for both transfer directions is equal to the distribution coefficient m :

$$\frac{c_{A,0}(d \rightarrow c)}{c_{A,0}(c \rightarrow d)} = m \quad (3)$$

With Eq. (3), the maximum amount of solute to be transported is equal in both cases. Due to the relatively low acetone concentration, the distribution coefficient was set constantly to 0.63. The drop formation and contact times for every drop diameter are given in Table 2. Since the volumetric flow rate is kept constant to avoid differences in the convection mass transfer, the drop formation time t_f increases with drop diameter. The contact time t_c is the sum of drop formation time, time between end of formation and release (0.2 s) and withdrawal time of the second pump.

Position of Table 1

Position of Table 2

3. Results and discussion

3.1 Extraction efficiency

Fig. 2 shows the extraction efficiency E for the mass transfer direction out of the drops ($d \rightarrow c$). The efficiency predicted by the models of Licht & Pansing [7] and Heertjes *et al.* [16] are given for comparison. The experimental data lie between both models. The models predict a local minimum of the efficiency for 3 mm drops which can also be found in the experimental data with $c_{A,0} < 30$ g/L. The efficiency increases with higher initial solute concentrations. This is clearly due to Marangoni convection induced flow patterns which promote radial mixing inside the drop. Visual observations reveal stronger lateral drop movement at the nozzle tip with higher solute concentrations (for very high concentrations this movement can be so strong that the drop releases before drop formation is finished). For $c_{A,0} = 30$ g/L, the efficiency reaches an almost constant value of 35% which is about 1.7 times higher than the lowest value for lower concentration considered. The local minimum vanishes. This can be an indication that Marangoni convection is now the predominant mechanism and independent of drop diameter.

Position of Fig. 2

The extraction efficiency for the mass transfer direction $c \rightarrow d$ is shown in Fig. 3. The first impression is that there is a less clear dependency on diameter and solute concentration. Anyway, the higher the initial concentration is the more effective is the extraction. For the highest initial concentration efficiencies up to 55% are possible which is about 1.5 times higher than for the reversed direction. Visual observations clearly indicate stronger drop swinging at the nozzle for $c \rightarrow d$ than for the reversed mass transfer direction. Obviously, Marangoni effects are indeed stronger during drop formation for the mass transfer

direction into the drop phase. But another effect occurs: in the mass transfer direction $c \rightarrow d$ coalescence is more inhibited. The coalescence inhibition for the mass transfer direction $c \rightarrow d$ has been observed by many researchers (e.g. [29-31]). This effect can be explained with the reduced film drainage between drop and dispersed phase at the Teflon tip due to Marangoni convection. From that it follows that the drops coalesce later than in the reverse direction, additionally, the coalescence time is somewhat random. The drop area is present for a longer time, additional mass transfer takes place and more mass can be transferred in same time range in the glass cylinder.

Position of Fig. 3

3.2 Correlation of total transferred mass

Fig. 4 shows the totally extracted ($d \rightarrow c$) resp. absorbed ($c \rightarrow d$) mass M_A as a function of drop diameter for all experiments (symbols). The total transferred mass increases with drop diameter and initial solute concentration. The lines ($d \rightarrow c$) and dashed lines ($c \rightarrow d$) have been calculated with:

$$M_A = \frac{6}{7} \cdot d_{p,f}^2 \Delta c_A \sqrt{t_c \pi} \sqrt{\alpha(c_{A,0})} D_A \quad (4)$$

with an initial concentration dependent diffusivity factor $\alpha(c_{A,0})$ obtained by simple regression analysis. The diffusivity factor accounts for the additional convection due to the Marangoni effect. Since these convection patterns are of isotropic nature similar to molecular diffusion, $\alpha(c_{A,0})$ is considered as a reasonable modification of the diffusion coefficient. The introduction of an effective diffusivity is subject to models in turbulent flows and to various mass transfer models, proposed to predict the mass transfer enhancement due to turbulence-like flow patterns or Marangoni effects in the free drop rise or fall stage (e.g. [8, 9, 26, 32, 33]).

The constant in Eq. (4) has been chosen arbitrarily to 6/7 according to the model of Licht & Pansing [7]. This model predicts the lowest transferred mass and is used as a reference. Note that in Eq. (4) the contact time t_c (see Table 2) has been used to account for the additional mass transfer during drop rise and coalescence until withdrawal.

Position of Fig. 4

The diffusivity factor $\alpha(c_{A,0})$ is shown in Fig. 5 as a function of initial solute concentration $c_{A,0}$ for both mass transfer directions. $\alpha(c_{A,0})$ increases linearly with initial solute concentration. The correlation coefficient is satisfying (0.97 for $c \rightarrow d$ and 0.99 for $d \rightarrow c$). The higher slope for the mass transfer direction $c \rightarrow d$ indicates that the diffusivity factor is more sensitive to the initial solute concentration in this direction. The linearity can possibly be explained with the interfacial tension gradient $\partial\sigma/\partial c_A$, which is the relevant driving force. In the concentration range considered in this study, the interfacial tension gradient changes almost linearly with solute concentration in the lower concentration range (up to 20 g/L, see [28]). Finally, Fig. 6 shows a parity plot of calculated and measured total transferred mass. As can be seen, the correlation (Eq. (4)) is satisfying within $\pm 30\%$.

Position of Fig. 5

Position of Fig. 6

4. Summary and conclusion

The impact of Marangoni convection on the mass transfer during drop formation has been investigated in the ternary system toluene/acetone/water. The extraction efficiency depends strongly on the initial solute concentration and mass transfer direction and reached up to 55% in the concentration range investigated here. Marangoni convection promotes internal mixing and enhances mass transfer. The mixing effect seems to be stronger with higher initial solute concentrations since higher interfacial tension gradients can occur. Visual observations of lateral drop movement at the nozzle tip support this assumption. An upper and lower limit for extraction efficiency has yet to be determined. Therefore, further investigations using lower and higher initial concentrations are needed.

Existing models cannot predict extraction efficiency since they are independent of the initial solute concentration. With the introduction of a single parameter, the diffusivity factor, the total transferred mass can be correlated with reasonable accuracy. The diffusivity factor is linearly proportional to the initial solute concentration for both mass transfer directions. It accounts for the turbulence-like convection flow patterns induced by Marangoni effects.

The role of coalescence remains unclear. Due to the experimental method chosen in this work, the impact of coalescence in general and of coalescence inhibition in the special case $c \rightarrow d$ are inherently included in all considerations. Experimental investigations are necessary to deduce the impact of coalescence phenomena on total mass transfer.

Acknowledgement

We thank Gregor Bernutz for performing most of the experiments. Financial support provided by the German Research Foundation (DFG) is gratefully acknowledged.

References

- [1] W. Licht, J.B. Conway, Mechanism of Solute Transfer in Spray Towers, *Industrial and Engineering Chemistry* 42 (6) (1950) 1151-1157.
- [2] A.H.P. Skelland, S.S. Minhas, Dispersed Phase Mass Transfer During Drop Formation and Coalescence in Liquid-Liquid Extraction, *AIChE Journal* 17 (6) (1971) 1316-1324.
- [3] W.J. Heideger, M.W. Wright, Liquid extraction during drop formation: Effect of formation time. *AIChE Journal* 32 (8) (1986) 1372-1376.
- [4] A. Kumar, S. Hartland, Correlations for prediction of mass transfer coefficients in single drop systems and liquid-liquid extraction columns, *Chemical Engineering Research & Design* 77 (A5) (1999) 372-384.
- [5] W. Mensing, K. Schügerl, Stoffaustauschmessungen an schwebenden Tropfen. Teil II: Meßergebnisse, *Chemie Ingenieur Technik - CIT* 42 (15) (1970) 991-995.

- [6] F.B. West, P.A. Robinson, A.C. Morgenthaler, T.R. Beck, D.K. McGregor, Liquid-Liquid Extraction from Single Drops, *Industrial and Engineering Chemistry* 43 (1) (1951) 234-238.
- [7] W. Licht, W.F. Pansing, Solute Transfer from Single Drops in Liquid-Liquid Extraction, *Industrial and Engineering Chemistry* 45 (9) (1953) 1885-1896.
- [8] T.B. Liang, M.J. Slater, Liquid-liquid extraction drop formation: mass transfer and the influence of surfactant, *Chemical Engineering Science* 45 (1) (1990) 97-105.
- [9] L. Steiner, G. Oezdemir, S. Hartland, Single-Drop Mass Transfer in the Water-Toluene-Acetone System, *Ind. Eng. Chem. Res.* 29 (1990), 1313-1318.
- [10] A. Javadi, D. Bastani, M. Taeibi-Rahni, Mass transfer during drop formation on the nozzle: New flow expansion model, *AIChE Journal* 52 (3) (2006), 895-910.
- [11] D.S. Walia, D. Vir, Extraction from single forming drops, *The Chemical Engineering Journal* 12 (2) (1976) 133-141.
- [12] P.M. Heertjes, L.H. de Nie, The mechanism of mass transfer during formation, release and coalescence of drops. Part I--Mass transfer to drops formed at a moderate speed, *Chemical Engineering Science* 21 (9) (1966) 755-768.
- [13] H. Groothuis, H. Kramers, Gas absorption by single drops during formation, *Chemical Engineering Science* 4 (1955) 17.
- [14] D. Ilkovic, Polarographic studies with the dropping mercury cathode, *Coll. Czech. Chem. Commun.* 6 (1934) 498.
- [15] H.H. Michels, The mechanisms of mass transfer during bubble formation, Ph.D. Thesis, University of Delaware, 1960.
- [16] P.M. Heertjes, W.A. Holve, H. Talsma, Mass transfer between isobutanol and water in a spray-column, *Chemical Engineering Science* 3 (3) (1954) 122-142.
- [17] A.T. Popovich, R.E. Jarvis, O. Trass, Mass transfer during single drop formation, *Chemical Engineering Science* 19 (5) (1964) 357-365.
- [18] M.J. Slater, M.H.I. Baird, T.B. Liang, Drop phase mass transfer coefficients for liquid-liquid systems and the influence of packings, *Chemical Engineering Science* 43 (2) (1988) 233-245.
- [19] J.D. Thornton, T.J. Anderson, K.H. Javed, S.K. Achwal, Surface Phenomena and Mass Transfer Interactions in Liquid-Liquid Systems. Part I: Droplet Formation at a Nozzle, *AIChE Journal*, 31 (7) (1985) 1069-1076.
- [20] J. Thornton, Interfacial Phenomena and Mass-Transfer in Liquid-Liquid-Extraction, *Chemistry & Industry* 6 (1987), 193-196.
- [21] K.H. Javed, J.D. Thornton, T.J. Anderson, Surface phenomena and mass transfer rates in liquid-liquid systems: Part 2, *AIChE Journal* 35 (7) (1989) 1125-1136.
- [22] D. Agble, M.A. Mendes-Tatsis, The effects of surfactants on Marangoni convection in the Isobutanol/Water System, *Journal of Non-Equilibrium Thermodynamics* 25 (3/4) (2000) 239-249.
- [23] D. Agble, M.A. Mendes-Tatsis, The effect of surfactants on interfacial mass transfer in binary liquid-liquid systems, *International Journal of Heat and Mass Transfer* 43 (6) (2000) 1025-1034.
- [24] D. Agble, M.A. Mendes-Tatsis, The prediction of Marangoni convection in binary liquid-liquid systems with added surfactants, *International Journal of Heat and Mass Transfer* 44 (7) (2001) 1439-1449.
- [25] B. Arendt, R. Eggers, Interaction of Marangoni convection with mass transfer effects at droplets, *International Journal of Heat and Mass Transfer*, 50 (13-14) (2007) 2805-2815.

- [26] M. Henschke, A. Pfennig, Mass-Transfer Enhancement in Single-Drop Extraction Experiments, *AICHe Journal* 45 (10) (1999) 2079-2086.
- [27] M. Wegener, J. Grünig, J. Stüber, A.R. Paschedag, M. Kraume, Transient rise velocity and mass transfer of a single drop with interfacial instabilities - experimental investigations, *Chemical Engineering Science* 62 (11) (2007) 2967-2978.
- [28] T. Misek, R. Berger, J. Schröter, Standard test systems for liquid extraction, *Inst. Chem. Eng., EFCE Publication Series* 46 (1985).
- [29] E. Bender, R. Berger, W. Leuckel, D. Wolf, D., Untersuchungen zur Betriebscharakteristik pulsierter Füllkörperkolonnen für die Flüssig/Flüssig-Extraktion, *Chemie Ingenieur Technik* 51 (3) (1979) 192-199.
- [30] K.-H. Reissinger, R. Marr, Auslegungskonzept für pulsierte Siebboden-Extraktoren, *Chemie Ingenieur Technik* 58 (7) (1986) 540-547.
- [31] B. Hoting, A. Vogelpohl, Untersuchungen zur Fluidodynamik und Stoffübertragung in Extraktionskolonnen mit strukturierten Packungen Teil II: Einfluß der Stoffübertragung auf das fluiddynamische Verhalten und erzielbare Trennleistungen, *Chemie Ingenieur Technik - CIT* 68 (1-2) (1996) 109-113.
- [32] P.H. Calderbank, I.J.O. Korchinski, Circulation in liquid drops: (A heat-transfer study), *Chemical Engineering Science* 6 (2) (1956) 65-78.
- [33] A.E. Handlos, T. Baron, Mass and Heat Transfer from Drops in Liquid-Liquid Extraction, *AICHe Journal* 3 (1) (1957) 127-136.

Figure captions

- Fig. 1: Experimental setup for drop formation experiments. (1) glass column, ID = 50 mm, (2) Teflon tip embedded in glass cylinder, ID = 5 mm, (3) glass nozzle, ID = 0.5 mm, (4) solenoid device, (5) precision dosing pumps, (6) computer control, (7) storage vial, (8) sample vial, (9) drop.
- Fig. 2: Extraction efficiency E for the mass transfer direction $d \rightarrow c$ as a function of drop diameter. The models of Heertjes *et al.* (1954) and Licht & Pansing (1953) are given for comparison.
- Fig. 3: Extraction efficiency E for the mass transfer direction $c \rightarrow d$ as a function of drop diameter. The models of Heertjes *et al.* (1954) and Licht & Pansing (1953) are given for comparison.
- Fig. 4: Total transferred mass M_A as a function of drop diameter for both mass transfer directions. Symbols: experiments, solid lines and dashed lines: calculated with Eq. (4)
- Fig. 5: Diffusivity factor as a function of initial solute concentration for both mass transfer directions.
- Fig. 6: Parity plot of measured and calculated total transferred mass. For the calculations, Eq. (4) has been used.

Tables

Table 1: Performed measurements

$d_p = 2, 2.5, 3, 3.5, 4 \text{ mm}$	
$d \rightarrow c: c_{A,0}$	$c \rightarrow d: c_{A,0}$
[g/L]	[g/L]
1.8	2.9
3.7	5.9
7.5	12
15	24
30	49

Table 2: Formation and contact times

d_p [mm]	2.0	2.5	3.0	3.5	4.0
t_f [s]	0.65	1.06	1.48	2.42	3.47
t_c [s]	2.42	3.19	4.26	6.03	8.16

Figures

Figure 1:

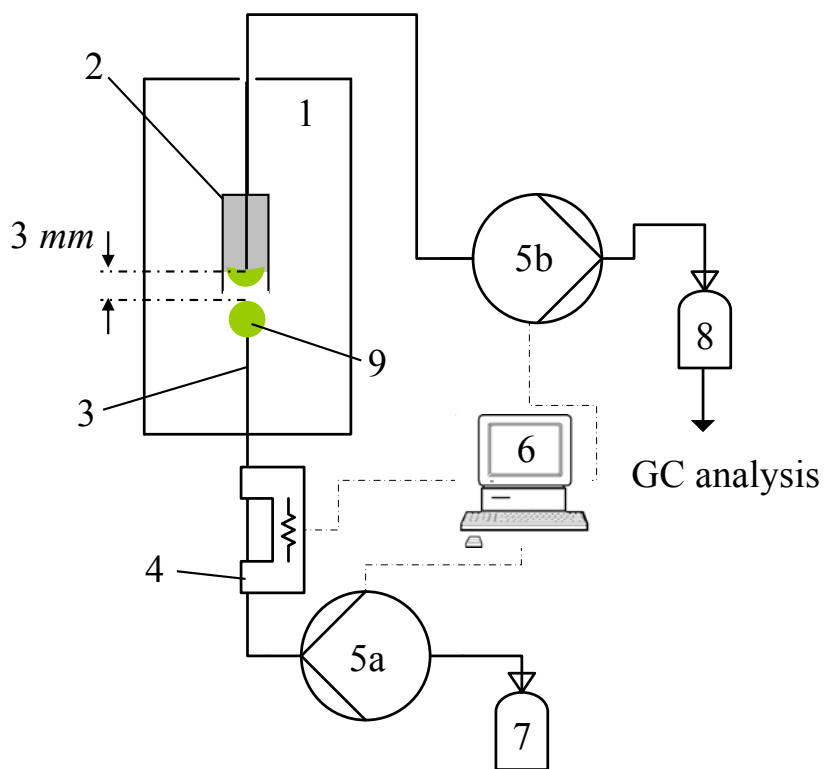


Figure 2:

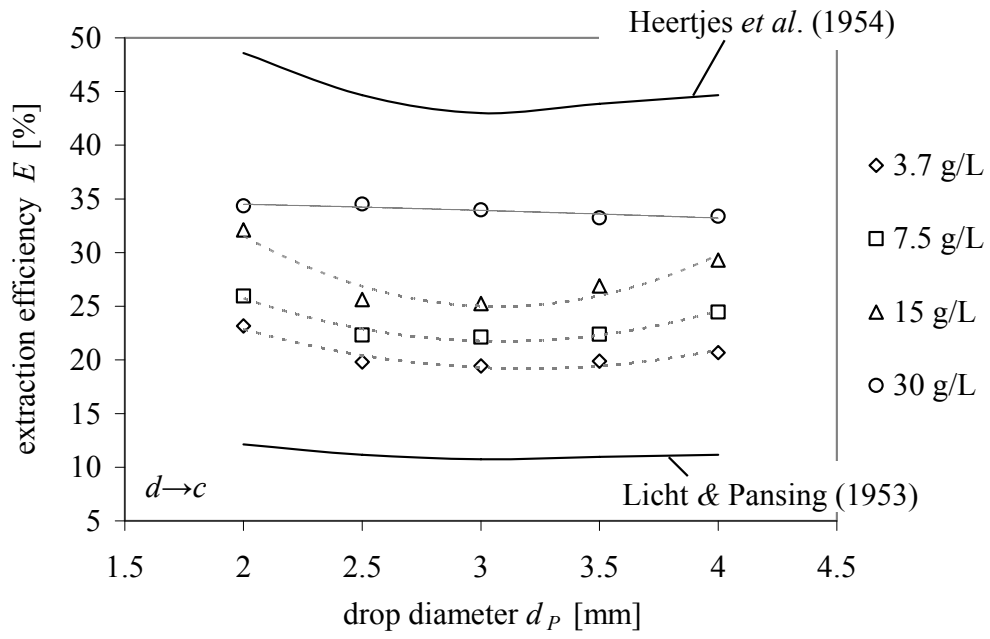


Figure 3:

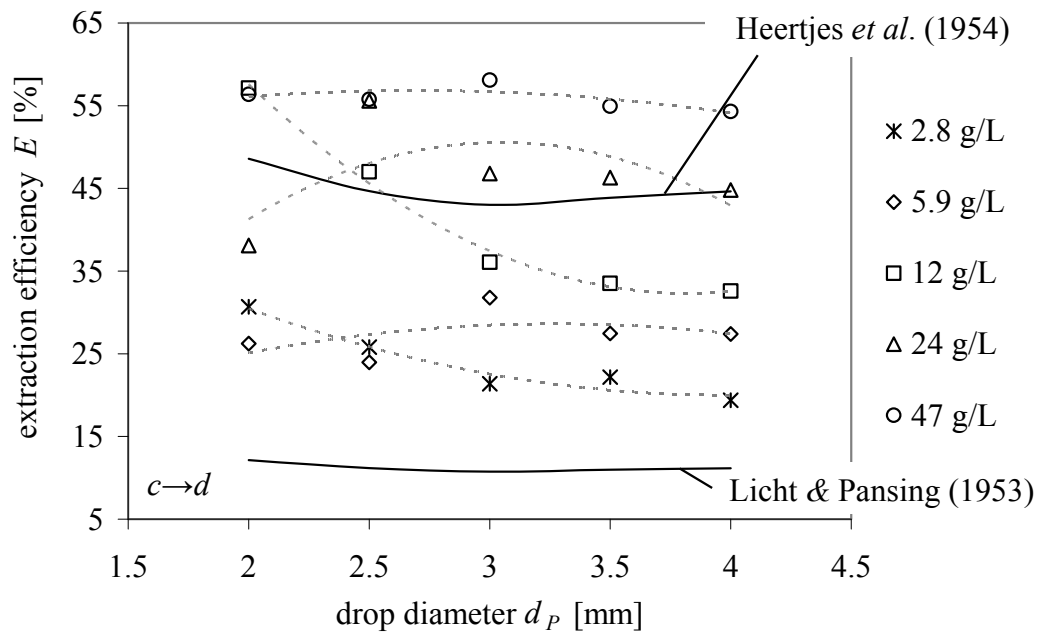


Figure 4:

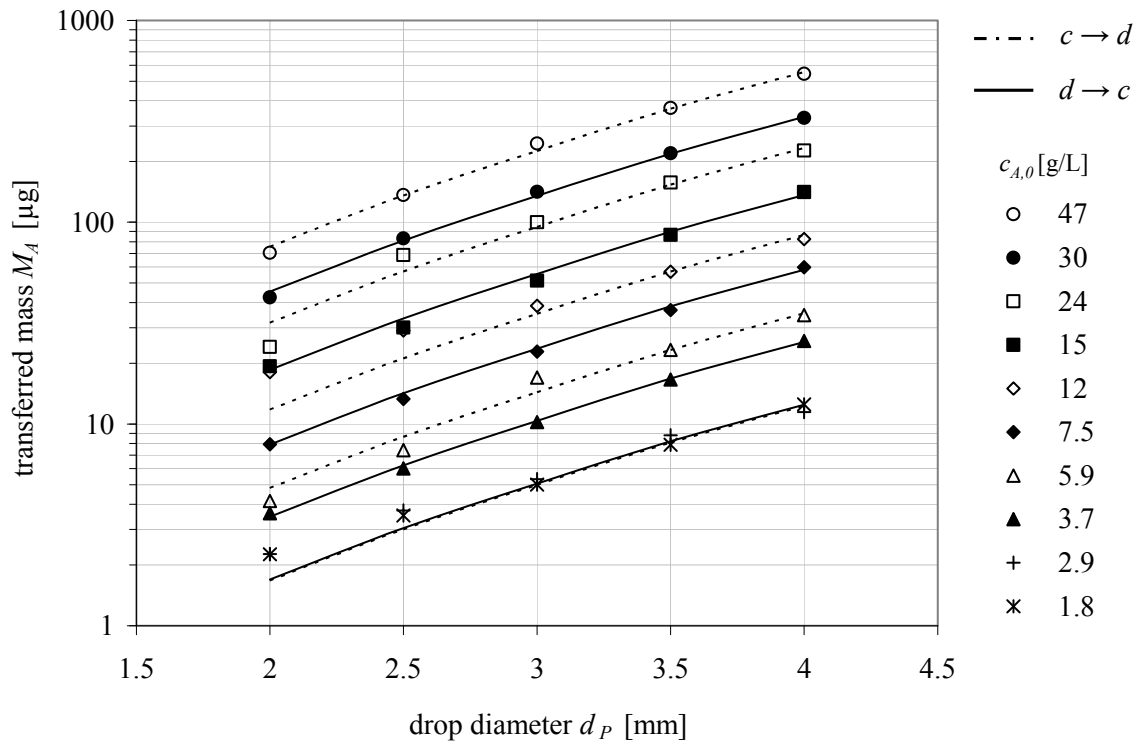


Figure 5:

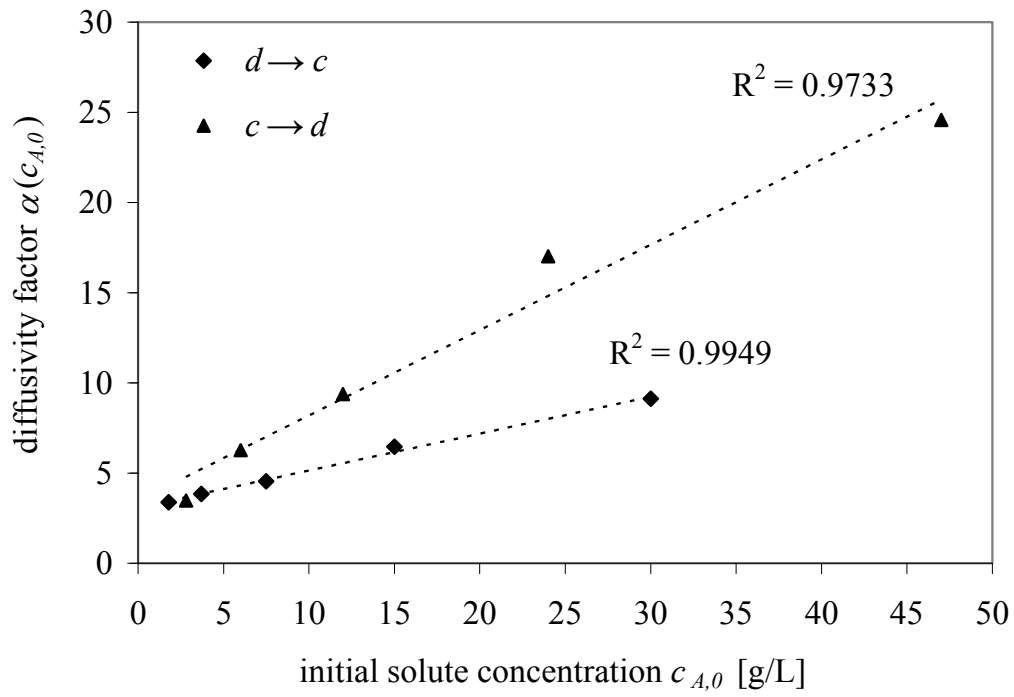


Figure 6:

